Transition Metal Complexes with Sulfur Ligands, 143[‡]

Coordination of CO, NO, N_2H_2, and Other Nitrogenase Relevant Small Molecules to Sulfur-Rich Ruthenium Complexes with the New Ligand 'tpS_4'$^{2-}$ = 1,2-Bis(2-mercaptophenylthio)phenylene(2–)

Dieter Sellmann,*[a] Klaus Engl,[a] Frank W. Heinemann,[a] and Joachim Sieler[b]

Dedicated to Professor Heinrich Vahrenkamp on the occasion of his 60th birthday

Keywords: Ruthenium / S ligands / Hydrazine / Diazene

In the search for ruthenium complexes with sulfur-dominated coordination spheres that bind, activate, or stabilize nitrogenase relevant molecules, complexes containing the new and robust tetradentate ligand 'tpS_4'–H_2 were synthesized. Treatment of $[RuCl_2(PPh_3)_3]$ with 'tpS_4'$^{2-}$ gives $[Ru(PPh_3)_2('tpS_4')]$ (**1**), which contains two labile PPh_3 ligands. The reaction of **1** with PEt_3 or DMSO led to substitution of both PPh_3 ligands, yielding $[Ru(PEt_3)_2('tpS_4')]$ (**2**) and $[Ru(DMSO)_2('tpS_4')]$ (**3**), respectively. When treated with nitrogenous ligands, complex **1** lost only one PPh_3 ligand to yield $[Ru(L)(PPh_3)('tpS_4')]$ complexes where L = py (**7**), NH_3 (**8**), N_2H_4 (**9**), NH_2NHMe (**10**), and CH_3CN (**12**), all of which are labile. The labile acetonitrile complex $[Ru(CH_3CN)(PPh_3)('tpS_4')]$ (**12**) proved to be particularly suited as a precursor for the syntheses of other $[Ru(L)(PPh_3)('tpS_4')]$ complexes. The 18 and 19 valence electron NO complexes $[Ru(NO)(PPh_3)('tpS_4')]BF_4$ (**13**) and $[Ru(NO)(PPh_3)('tpS_4')]$ (**14**), $(NEt_4)[Ru(N_3)(PPh_3)('tpS_4')]$ (**15**), $[Ru(I)(PPh_3)('tpS_4')]$ (**16**), and $[Ru(N_3)(PPh_3)('tpS_4')]$ (**17**) were obtained starting from complex **12**. The labile mononuclear hydrazine complex $[Ru(N_2H_4)(PPh_3)('tpS_4')]$ (**9**) gave the dinuclear complex $[\mu\text{-}N_2H_4\{Ru(PPh_3)('tpS_4')\}_2]$ (**18**) by dissociation of hydrazine. The dinuclear diazene complex $[\mu\text{-}N_2H_2\{Ru(PPh_3)('tpS_4')\}_2]$ (**19**) was obtained by oxidation of **9** and more readily from $[Ru(CH_3CN)(PPh_3)('tpS_4')]$ (**12**) and N_2H_2, which was generated in situ from $K_2N_2(CO_2)_2$ and acetic acid. The molecular structures of **7**, **13**, **16**, **18**, and **19** were determined by X-ray structure analyses. The complexes **18** and **19** represent the first complexes containing the hydrazine/diazene couple, which enables us to compare both the bonding features and the formation of N–H···S bridges when hydrazine and diazene bind to transition metal sulfur sites.

Introduction

The stabilization, or coordination and activation of small molecules such as CO, N_2, H_2, NO, N_3^-, N_2H_2, N_2H_4, and NH_3 by transition metal sulfur complexes is of pivotal interest for understanding the molecular mechanisms of nitrogenases.[1] It can be assumed that these molecules interact with the FeMo, FeV, or FeFe cofactors that are the active sites of nitrogenases. The FeMo cofactors of FeMo nitrogenase in the resting state have been shown by X-ray crystallography to contain $[Fe_7MoS_9]$ clusters.[2] Similar structures are assumed for the FeV or FeFe cofactors of the alternative FeV and FeFe nitrogenases.[3] However, the functioning of these clusters has remained unexplained, not least because a compound that models basic structural *and* functional principles of the cofactors has yet to be found. In particular, these principles are metal sulfur sites *and* the mild catalytic reduction of N_2 with biologically compatible redox potentials.[4]

In our search for such compounds we have found that both the [Ru('S_4')] fragments and their tertiary butyl derivatives [Ru('$^{bu}S_4$')] coordinate the complete series of above mentioned molecules, with the exception of N_2 (Scheme 1).[5]

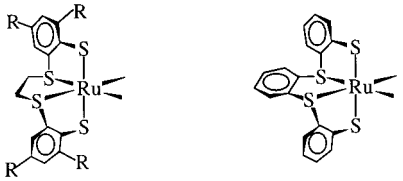

Scheme 1. [Ru('$^{R}S_4$')] and [Ru('tpS_4')]

Another shortcoming of the [Ru('$^{R}S_4$')] complexes are ligand C–S cleavage reactions. In most cases, the [Ru('$^{R}S_4$')] fragments prove to be robust and the '$^{R}S_4$'$^{2-}$ ligands stay intact, behaving as spectator ligands. However, under strongly reducing or photolytic conditions, in reactions with

[‡] Part 142: D. Sellmann, K. Engl, F. W. Heinemann, *Eur. J. Inorg. Chem.*, in press.

[a] Institut für Anorganische Chemie der Universität Erlangen-Nürnberg,
Egerlandstraße 1, 91058 Erlangen, Germany
Fax: (internat.) + 49-9131/852-7367
E-mail: sellmann@anorganik.chemie.uni-erlangen.de
[b] Institut für Anorganische Chemie der Universität Leipzig,
Linnéstraße 3, 04103 Leipzig, Germany

  1434–1948/00/0505–1079 $ 17.50+.50/0

electron-rich metal complexes, and in reactions involving 19 valence electron complexes, C(alkyl)–S cleavage reactions take place yielding, among other products, 1,2-benzenedithiolate, or vinylthio(2-mercapto)benzene(1–) ligands and ethylene.[6] Since aromatic C–S bonds are more stable towards cleavage than C(alkyl)–S bonds, we synthesized the new dithioether–dithiolate ligand 'tpS_4'$^{2-}$ = 1,2-bis(2-mercaptophenylthio)phenylene(2–), which contains exclusively aromatic C–S bonds. In a previous paper we described the syntheses of 'tpS_4'$^{2-}$ and a few Ru, Os, and Ni complexes containing [M('tpS_4')] fragments, demonstrating that the 'tpS_4'$^{2-}$ ligand coordinates metals in the same helical manner as the '$^{R}S_4$'$^{2-}$ ligands and is indeed stable toward C–S cleavage.[7] Preliminary tests also indicated that analogous [Ru('$^{R}S_4$')] and [Ru('tpS_4')] complexes can have quite different substitution reactivity. This prompted us to systematically investigate the synthesis and reactivity of [Ru('tpS_4')] complexes, focusing on hydrazine, nitrosyl, and azido derivatives as potential N_2 complex precursors,[8] because subtle differences in the [Ru('$^{R}S_4$')] and [Ru('tpS_4')] fragments may be decisive in the binding or nonbinding of N_2.[9]

Results

Syntheses of [Ru('tpS_4')] Complexes with DMSO, Phosphanes, and Nitrogenous Coligands

In the search for labile [Ru(L)(L')('tpS_4')] complexes we probed the exchange of PPh_3 in the readily accessible [Ru(PPh_3)$_2$('tpS_4')] (**1**) (Scheme 2).[7]

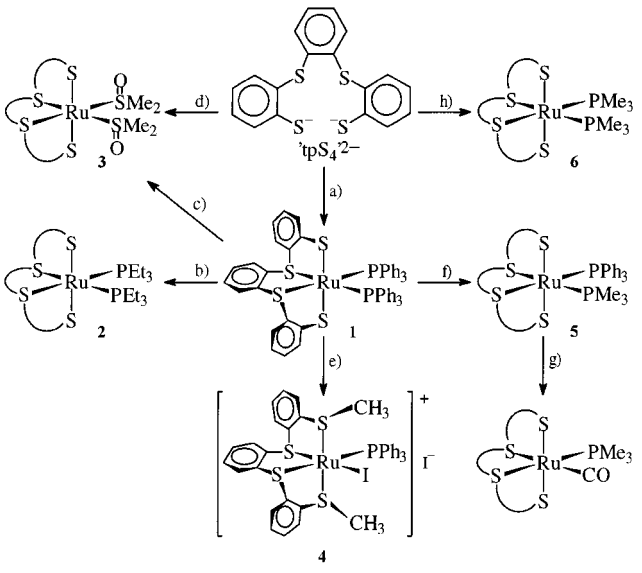

Scheme 2. Phosphane and DMSO exchange reactions of [Ru(PPh_3)$_2$('tpS_4')]: a) + [$RuCl_2(PPh_3)_3$], THF, 4 h, room temperature (room temp.); b) + exc. PEt_3, THF, 3 min, reflux; c) DMSO, 5 min, reflux; d) + [$RuCl_2(DMSO)_4$], THF, 2.5 d, room temp.; e) + CH_3I, 2 h, room temp.; f) + exc. PMe_3, THF, 3 h, room temp.; g) + CO (1bar), THF, 4 d, room temp.; h) + [$RuCl_2(PMe_3)_4$], MeOH, 4 h, reflux

When **1** was treated with PEt_3, [Ru(PEt_3)$_2$('tpS_4')] (**2**) formed. Formation of the mixed phosphane complex [Ru(PEt_3)(PPh_3)('tpS_4')] was not observed. Brief heating of **1** in DMSO yielded [Ru(DMSO)$_2$('tpS_4')] (**3**) which could be readily obtained directly from [$RuCl_2(DMSO)_4$] and 'tpS_4'$^{2-}$. With regard to the PEt_3 and DMSO reactions, the reactivity of **1** is in contrast to that of the parent complex [Ru(PPh_3)$_2$('S_4')] which exchanges only one or none of its PPh_3 ligands under comparable conditions. An analogous behavior of **1** and the parent complex [Ru(PPh_3)$_2$('S_4')] was found in the reactions with MeI and PMe_3. Treatment of **1** in CH_2Cl_2 with excess MeI afforded the doubly methylated derivative [Ru(I)(PPh_3)('tpS_4–Me_2')]I (**4**) in isomerically pure form. PMe_3 was able to substitute only one PPh_3 ligand in **1** to give [Ru(PMe_3)(PPh_3)('tpS_4')] (**5**), even when an excess of PMe_3 was applied and the temperature was raised. The bis(PMe_3) complex [Ru(PMe_3)$_2$('tpS_4')] (**6**) formed from [$RuCl_2(PMe_3)_4$] and Li_2–'tpS_4' in boiling MeOH.

In order to probe the lability of PMe_3 versus that of PPh_3 in [Ru(PMe_3)(PPh_3)('tpS_4')] (**5**), complex **5** was treated with CO under standard conditions. Monitoring the reaction by IR and NMR spectroscopy as well as mass spectrometry showed the formation of [Ru(CO)(PMe_3)('tpS_4')], indicating that in **5** the large PPh_3 is more labile than the small PMe_3 ligand.

The complexes **2**–**6** proved to be less labile than the PPh_3 complex **1** and were not suited for exchange reactions with nitrogenous ligands. Attempts to exchange directly one PPh_3 in **1** for such ligands succeeded with pyridine, hydrazine(s), ammonia, and even diazomalonic ethyl ester, but failed for NO, NO^+, or N_3^-. In order to achieve their coordination it was necessary to proceed via the acetonitrile complex [Ru(MeCN)(PPh_3)('tpS_4')] (**12**). Scheme 3 summarizes these reactions and complexes.

Brief heating of **1** in pyridine gave [Ru(py)(PPh_3)('tpS_4')] (**7**). Treatment of **1** in THF with an excess of NH_3 gas, N_2H_4, or N_2H_3Me likewise afforded [Ru(NH_3)(PPh_3)('tpS_4')] (**8**), [Ru(N_2H_4)(PPh_3)('tpS_4')] (**9**), and [Ru(N_2H_3Me)(PPh_3)('tpS_4')] (**10**). In order to drive the reactions to completion, the solutions were usually heated to boiling for a short time. The conversion of **9** into a dinuclear hydrazine complex is described below.

A reaction was also observed between **1** and diethyl diazomalonate [$N_2C(CO_2Et)_2$)] in boiling THF. Monitoring the reaction by ^1H NMR spectroscopy showed that the primary product is presumably [Ru{$N_2C(CO_2Et)_2$}(PPh_3)('tpS_4')], which rapidly transforms into the carbene complex [Ru{$C(CO_2Et)_2$}(PPh_3)('tpS_4')] (**11**).

These results indicate that nitrogenous ligands are able to selectively substitute one PPh_3 in [Ru(PPh_3)$_2$('tpS_4')] (**1**). In the quest for labile solvent complex derivatives of **1**, which had so far remained inaccessible, we now tried to obtain the acetonitrile complex [Ru(MeCN)(PPh_3)('tpS_4')] (**12**). The yellow complex **12** formed from boiling acetonitrile solutions of **1**, could be isolated in solid state, completely characterized, and proved an excellent starting material for further complexes.

The reaction of **12** with CO at ambient conditions established the lability of the MeCN ligand. The CO complex

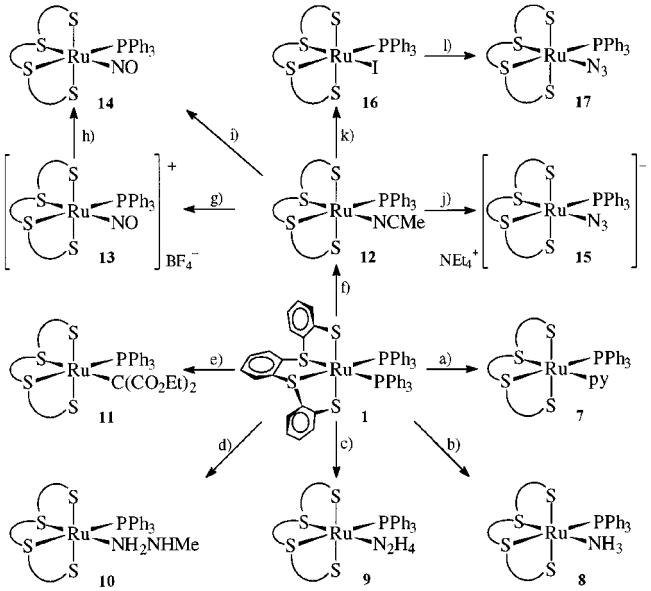

Scheme 3. Coordination of nitrogenous ligands to the [Ru(PPh$_3$)('tpS$_4$')] fragment: a) pyridine, 10 min, reflux; b) + NH$_3$ (gaseous), THF, 5 min, reflux; c) + exc. N$_2$H$_4$, THF, 10 min, reflux; d) + exc. NH$_2$NHMe, THF, 45 min, reflux; e) +exc. N$_2$C(CO$_2$Et)$_2$, THF, 4 h, reflux; f) MeCN, 3 h, reflux; g) + NOBF$_4$, CH$_2$Cl$_2$, 3 h, room temp.; h) + LiBEt$_3$ H, THF, 30 min, room temp.; i) NO (gaseous), CH$_2$Cl$_2$, 20 h, room temp.; j) + NEt$_4$N$_3$, acetone, 3 h, room temp.; k) + 0.5 I$_2$, THF 12 h, room temp.; l) + exc. NEt$_4$N$_3$, acetone, 3 d, room temp.

[Ru(CO)(PPh$_3$)('tpS$_4$')] [ν(CO) = 1964 cm^{-1}] formed nearly instantly. [Ru(CO)(PPh$_3$)('tpS$_4$')] also formed directly from **1** and CO. However, this reaction needed ca. 12 h to go to completion.[7]

Treatment of **12** with one equivalent of NOBF$_4$ yielded [Ru(NO)(PPh$_3$)('tpS$_4$')]BF$_4$ (**13**). Complex **13** is the first 18 valence electron nitrosyl complex with an [RuPS$_4$] core characterized by X-ray structure determination. It was of particular interest as a test complex for probing the stability of the 'tpS$_4$'$^{2-}$ ligand towards reduction.

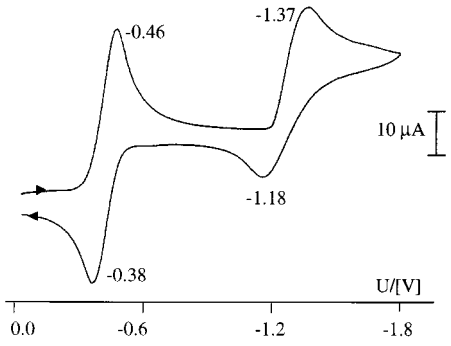

Figure 1. Cyclic voltammogram of [Ru(NO)(PPh$_3$)('tpS$_4$')]BF$_4$ (**13**) in CH$_2$Cl$_2$ (10^{-3} M, 10^{-1} M NBu$_4$PF$_6$, v = 0.05Vs^{-1})

The cyclic voltammogram (CV) of **13** in CH$_2$Cl$_2$ (Figure 1) exhibited two redox waves in the cathodic region. The redox wave at $E_{1/2}$ = –0.42 V could be assigned to the reversible reduction [Ru(NO)(PPh$_3$)('tpS$_4$')]$^+$/[Ru(NO)(PPh$_3$)('tpS$_4$')]^0 and indicated the viability of the neutral 19 valence electron nitrosyl complex [Ru(NO)(PPh$_3$)('tpS$_4$')] (**14**).

This result was corroborated by chemical reduction of **13** and the reaction of the acetonitrile complex **12** with NO gas. Monitoring the reaction of **13** with LiBEt$_3$H in THF by IR spectroscopy showed that the ν(NO) band of **13** at 1850 cm^{-1} was replaced by a new band at 1602 cm^{-1}. No gas was evolved, and the intensity and frequency of the 1602 cm^{-1} band was found to be compatible with the formation of **14**.[10] Treating **12** with NO gas in CH$_2$Cl$_2$ led to a strong ν(NO) band appearing in the same region at 1605 cm^{-1}. Complex **14** could be precipitated from this solution as red-brown solid by the addition of *n*-hexane. Complex **14** is highly reactive and almost instantly oxidized by traces of air to give the [Ru(NO)(PPh$_3$)('tpS$_4$')]$^+$ cation, as indicated by the ν(NO) band at 1842 cm^{-1} (KBr). Complex **14** is paramagnetic and was only characterized by elemental analyses, IR spectroscopy, and mass spectrometry, which confirmed that the 'tpS$_4$'$^{2-}$ ligand remained intact.

Attempts to convert the nitrosyl ligands of either cationic **13** or neutral **14** into dinitrogen ligands by reactions with azide or ammonia have so far been unsuccessful. For the alternate route, in which the ligating azide is converted into N$_2$ by attack with NO$^+$, azido complexes were needed. Treatment of **12** in acetone with one equivalent of NEt$_4$N$_3$ yielded the azido complex (NEt$_4$)[Ru(N$_3$)(PPh$_3$)('tpS$_4$')] (**15**) whose formation could be established by IR and ^{1}H NMR spectroscopy. However, **15** proved to be too labile to obtain ^{13}C and ^{31}P NMR spectra and rapidly decomposed, even in the solid state, to give a brown mixture of intractable products. Repeated attempts to purify **15** by recrystallization were unsuccessful. For these reasons, we tried to obtain a potentially more stable Ru^{III} azide complex via the Ru^{III} iodide complex [Ru(I)(PPh$_3$)('tpS$_4$')] (**16**). Complex **16** formed from the reaction of the acetonitrile complex **12** with half an equivalent of iodine, and could be characterized by X-ray crystallography. The subsequent reaction of **16** with NEt$_4$N$_3$ yielded [Ru(N$_3$)(PPh$_3$)('tpS$_4$')] (**17**) which was isolated in pure state and characterized by IR spectroscopy and mass spectrometry. As expected, and confirmed from the ^{1}H NMR spectra showing broad and unresolved peaks, **16** and **17** are both paramagnetic. Complex **17** was further characterized by its cyclic voltammogram (Figure 2).

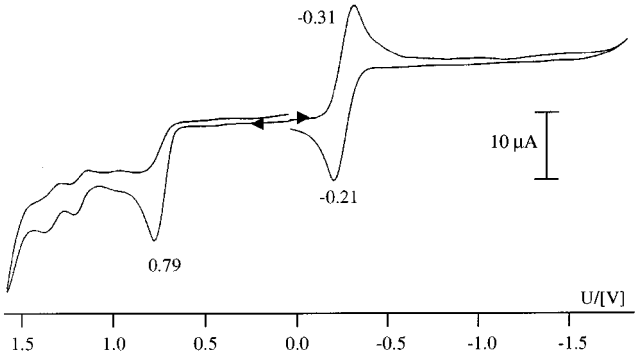

Figure 2. Cyclic voltammogram of [Ru(N$_3$)(PPh$_3$)('tpS$_4$')]BF$_4$ (**17**) in CH$_2$Cl$_2$ (10^{-3} M, 10^{-1} M NBu$_4$PF$_6$, v = 0.02Vs^{-1})

In the cathodic region, **17** showed a reversible redox wave at $E_{1/2}$ = –0.26 V. It is compatible with the reversible reduc-

tion of **17** to give the anion of the Ru^{II} complex **15**. Attempts to convert **17** photolytically, thermally, or by treatment with HBF_4 in CH_2Cl_2 into a dinitrogen complex remained unsuccessful.

Dinuclear Hydrazine and Diazene Complexes with [Ru(PPh$_3$)('tpS$_4$')] Fragments

The unsuccessful attempts to obtain a [Ru(PPh_3)('tpS_4')] dinitrogen complex via nitrosyl or azide precursors prompted us to return to the hydrazine complex [Ru(N_2H_4)(PPh_3)('tpS_4')] (**9**). As mentioned above, the N_2H_4 ligand is labile. In this respect **9** resembles the other [Ru(L)(PPh_3)('tpS_4')] complexes in which L is a σ-N donor ligand.

The complex [Ru(N_2H_4)(PPh_3)('tpS_4')] (**9**) did not yield a dinitrogen complex either. However, further investigation led to the characterization of [μ-N_2H_4{Ru(PPh_3)('tpS_4')}$_2$] (**18**) and [μ-N_2H_2{Ru(PPh_3)('tpS_4')}$_2$] (**19**) which represent the first hydrazine and diazene couple characterized by X-ray structure determination (Scheme 4).

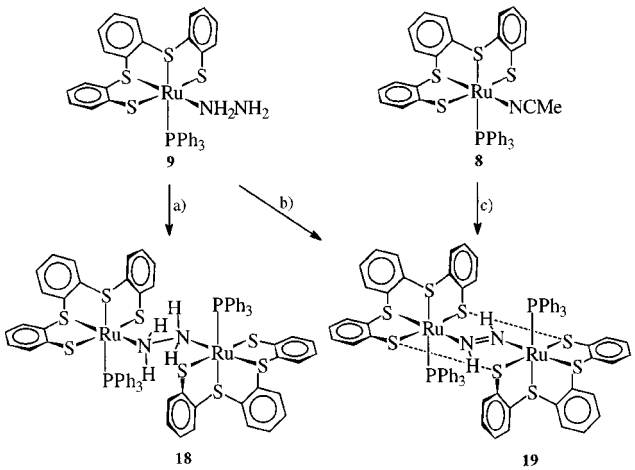

Scheme 4. Formation of dinuclear hydrazine and diazene complexes with [Ru(PPh_3)('tpS_4')] fragments: a) CH_2Cl_2, 7 d, room temp.; b) + O_2, CH_2Cl_2, 36 h, room temp.; c) + exc. $K_2N_2(CO_2)_2$, + exc. CH_3CO_2H, THF, 3 h, room temp.

Attempts to recrystallize **9** from CH_2Cl_2/MeOH mixtures afforded yellow microcrystals that proved so sparingly soluble that no NMR spectra could be recorded. The elemental analyses and IR spectra indicated that two molecules of mononuclear **9** had formed the dinuclear hydrazine complex **18** by dissociation of hydrazine. Carrying out the same experiment in THF/Et_2O mixtures afforded single crystals of **18**·4THF, which could be structurally characterized. When the CH_2Cl_2 solutions of the hydrazine complex **9** were treated with atmospheric oxygen, their color turned from yellow to dark green and green crystals precipitated. They were also sparingly soluble, but we were able to record a ^1H NMR spectrum which exhibited a signal at δ = 14.59, indicative of an N_2H_2 ligand in a centrosymmetric dinuclear diazene complex of the type [μ-N_2H_2{Ru(PPh_3)('tpS_4')}$_2$] (**19**). Intense absorptions at 307 and 463 nm in the UV/Vis spectrum also suggested the formation of **19**, which was finally and unambiguously characterized by an X-ray crystal structure determination of **19**·4CH_2Cl_2.

The aerial oxidation of **9** afforded **19** in yields of 25%. A potential reason for the low yield is that the dinuclear hydrazine complex **18** must form before subsequent oxidation occurs to give **19**. Therefore we sought a better synthesis of **19** and found that much higher yields (> 80%) were obtained from the reaction of the labile acetonitrile complex **12** with N_2H_2, which was generated in situ by acidolysis of $K_2N_2(CO_2)_2$ with dilute acetic acid in THF. This trapping of the unstable diazene in solution is possible with particular metal sulfur complex fragments and was first discovered with the synthesis of [μ-N_2H_2{Fe(PPr_3)('S_4')}$_2$].[11]

General Properties and Spectroscopic Characterization of [Ru(L)(L')('tpS$_4$')] Complexes

As far as possible, all [Ru(L)(L')('tpS_4')] complexes have been characterized by the common spectroscopic methods and elemental analyses. The molecular structures of **7**, **13**, **16**, **18**, and **19** have been determined by X-ray structure analysis. All Ru^{II} complexes are diamagnetic, while the two Ru^{III} complexes are paramagnetic as indicated by their ^1H NMR spectra. The colors of the complexes range from yellow or orange (**1**–**12**), to green (**17**, **19**) and brown (**13**, **14**, **16**). All complexes, except the dinuclear species **18** and **19**, show moderate to good solubilities in CH_2Cl_2. The IR spectra of all complexes in KBr exhibit the typical absorptions of the [Ru('tpS_4')] fragment. A strong ν(CO) absorption at 1968 cm^{-1} and a strong δ(PCH) at 953 cm^{-1} characterize [Ru(CO)(PMe_3)('tpS_4')]. A ν(SO) band at 1015 cm^{-1} indicates sulfur coordination of DMSO in [Ru$(DMSO)_2$('tpS_4')] (**3**). Weak ν(NH) (3334, 3292, 3245, 3164 cm^{-1}) and ν(CN) (2271 cm^{-1}) bands readily identify [Ru(N_2H_4)(PPh_3)('tpS_4')] (**9**) and [Ru(MeCN)(PPh_3)('tpS_4')] (**12**) respectively. Strong ν(NO) bands at 1852 and 1598 cm^{-1} characterize the nitrosyl complexes **13** and **14**. The azide complexes **15** and **17** show characteristic ν(N_3) absorptions at 2029 and 2036 cm^{-1}. The ^1H NMR spectra of C_2-symmetric [Ru$(L)_2$('tpS_4')] complexes exhibit a typical set of six multiplets for the aromatic 'tpS_4' protons. This multiplet changes when the symmetry is lowered to C_1 in [Ru(L)(L')('tpS_4')] complexes. In all [Ru(L)(PPh_3)('tpS_4')] complexes, the 'tpS_4' multiplets are superimposed on the PPh_3 multiplets. Thus, the [Ru(L)(PPh_3)('tpS_4')] complexes usually are more readily identified by their ^{13}C and ^{31}P NMR spectra.

However, the ^1H NMR spectrum of [Ru(I)(PPh_3)('tpS_4–Me_2')]I (**4**) showed two singlets for the methyl groups, establishing that only one of several possible isomers had formed. The ^1H NMR spectra of **8** and **12** exhibited characteristic singlets at δ = 1.70 and 1.75, indicating the coordination of ammonia and acetonitrile. The hydrazine complex **9** gave rise to two multiplets at δ = 4.2 and 4.1 which are attributed to the Ru-bound NH_2 group, and a broad singlet at δ = 3.4 which is assigned to the terminal NH_2 group. The N_2H_2 singlet at δ = 14.59 is characteristic of the diazene complex [μ-N_2H_2{Ru(PPh_3)('tpS_4')}$_2$] (**19**). Complex **19** was further characterized by its UV/Vis spectrum, showing a strong absorption at 463 nm (ε = 8162 L

mol^{-1} cm^{-1}) which is characteristic of the 4c-6 e^- π bond system of [M=NH=NH=M] fragments (Figure 3).[12]

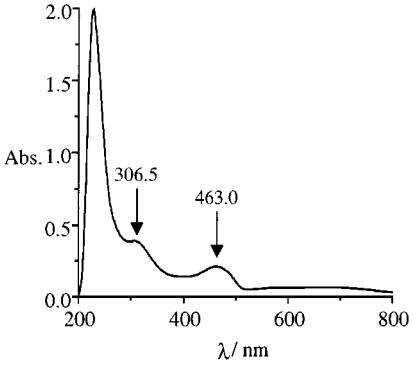

Figure 3. UV/Vis spectrum of $[\mu\text{–}N_2H_2\{Ru(PPh_3)(\text{'}tpS_4\text{'})\}_2]$ in CH_2Cl_2

X-ray Structure Analysis

The molecular structures of [Ru(py)(PPh_3)('tpS_4')] (**7**), [Ru(NO)(PPh_3)('tpS_4')]BF_4·CH_2Cl_2 (**13**·CH_2Cl_2), [Ru(I)(PPh_3)('tpS_4')]·CH_2Cl_2 (**16**·CH_2Cl_2), [μ-N_2H_4\{Ru(PPh_3)('tpS_4')\}$_2$]·4THF (**18**·4THF), and [μ-N_2H_2\{Ru(PPh_3)('tpS_4')\}$_2$]·4CH_2Cl_2 (**19**·4CH_2Cl_2) were determined by X-ray crystallography and are shown in Figure 4. Table 1 lists selected distances and angles.

In all cases the crystal lattices contain discrete molecules or ions. All compounds exhibit six-coordinate Ru centers, helical coordination of the 'tpS_4'$^{2-}$ ligands with *trans*-thiolate and *cis*-thioether S donors, and *cis* coordination of the ligands PPh_3 and L = py, NO, I, N_2H_4, N_2H_2.

Distances and angles lie in the range observed for related [Ru('S_4')] complexes. For example, in both the [Ru('tpS_4')] and [Ru('S_4')] complexes, the average Ru–S distances are found to be in the narrow range of 233–238 pm. This is worthy of note, in light of the different properties of the coligands which coordinate to the [RuS_4] cores, such as the σ-π ligands CO, NO^+ or N_2H_2, or the σ ligands N_2H_4 and pyridine. Even in the Ru^{III} complex [Ru(I)(PPh_3)('tpS_4')]·CH_2Cl_2 (**16**·CH_2Cl_2), the average Ru–S distance (234 pm) does not significantly differ from that of Ru^{II} complexes. This invariance of averaged M–S distances in low-spin complexes having no electrons in antibonding orbitals has been previously discussed and can be traced back to the bonding properties of sulfur ligands, which can function as σ-donor, σ-donor–π-acceptor, and σ-donor–π-donor ligands.[13–15]

The diazene and hydrazine complexes **19**·4CH_2Cl_2 and **18**·4THF deserve special consideration. They represent the first structurally characterized complexes containing the N_2H_2/N_2H_4 couple, and enable comparison of both the differing bonding situations and the formation of N–H···S bridges when hydrazine or diazene bind to transition metal

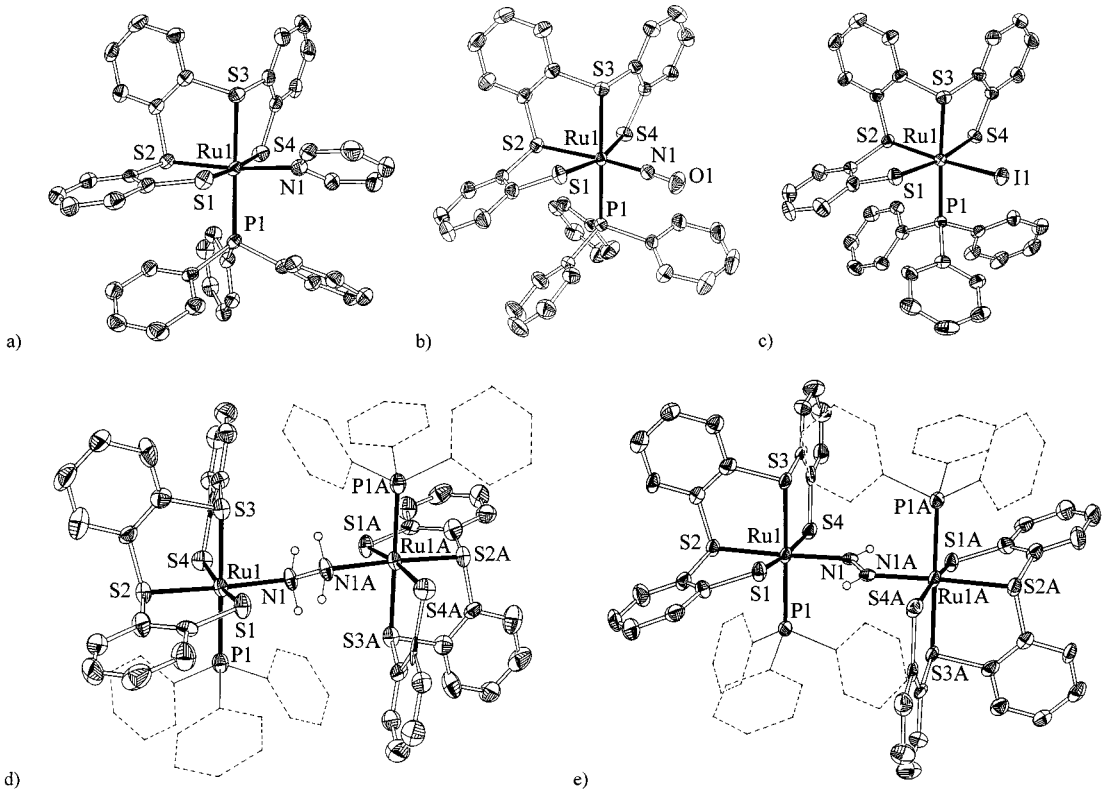

Figure 4. Molecular structures of a) [Ru(py)(PPh_3)('tpS_4')] (**7**), b) [Ru(NO)(PPh_3)('tpS_4')]BF_4·CH_2Cl_2 (**13**·CH_2Cl_2), c) [Ru(I)(PPh_3)('tpS_4')]·CH_2Cl_2 (**16**·CH_2Cl_2), d) [μ-N_2H_4\{Ru(PPh_3)('tpS_4')\}$_2$]·4THF (**18**·4THF), and e) [μ-N_2H_2\{Ru(PPh_3)('tpS_4')\}$_2$]·4CH_2Cl_2 (**19**·4CH_2Cl_2) (50% probability ellipsoids; C-bonded H atoms, solvent molecules, and BF_4^- anions omitted)

Table 1. Selected distances [pm] and angles [°] of [Ru(py)(PPh_3)('tpS_4')] (**7**), [Ru(NO)(PPh_3)('tpS_4')]BF_4·CH_2Cl_2 (**13**·CH_2Cl_2), [Ru(I)(PPh_3)('tpS_4')]·CH_2Cl_2 (**16**·CH_2Cl_2), [μ-N_2H_4{Ru(PPh_3)('tpS_4')$}_2$]·4THF (**18**·4THF), and [μ-N_2H_2{Ru(PPh_3)('tpS_4')$}_2$]·4CH_2Cl_2 (**19**·4CH_2Cl_2)

Complex (L)	**7** (py)	**13**·CH_2Cl_2 (NO^+)	**16**·CH_2Cl_2 (I)	**18**·4THF (N_2H_4)	**19**·4CH_2Cl_2 (N_2H_2)
Ru1–S1	238.5(1)	242.1(1)	236.0(2)	239.1(4)	239.8(2)
Ru1–S2	227.7(1)	239.1(1)	233.1(1)	227.5(4)	232.9(2)
Ru1–S3	234.1(1)	238.4(1)	234.2(1)	234.5(4)	234.5(2)
Ru1–S4	240.3(1)	236.2(1)	231.3(2)	239.4(4)	239.4(2)
Ru1–P1	234.5(1)	242.4(1)	237.7(2)	232.1(4)	235.8(2)
Ru1–L	215.5(3)	175.6(3)	271.18(6)	214.4(9)	203.0(7)
N1–N1A	–	–	–	149(2)	129(1)
N1–H1	–	–	–	102	88
S4–H1	–	–	–	298	289
S1A–H1	–	–	–	258	258
S3A–H2	–	–	–	288	–
S1–Ru1–S4	176.00(4)	165.45(4)	170.13(6)	171.9(1)	172.25(9)
S2–Ru1–S3	88.21(4)	86.49(3)	88.49(5)	88.6(1)	87.50(8)
S3–Ru1–P1	177.93(4)	174.88(3)	175.13(5)	179.8(2)	178.12(9)
S2–Ru1–P1	93.56(4)	91.91(3)	96.15(5)	91.6(1)	92.49(8)
S2–Ru1–L	172.42(10)	172.88(10)	169.19(4)	175.8(3)	175.8(2)
Ru1–N1–N1A	–	–	–	117.1(9)	127.4(7)
Ru1–N1–H1	–	–	–	112.3	121.7
N1–N1A–H1	–	–	–	97.2	110.9

sulfur sites. Both complexes possess a crystallographically imposed inversion symmetry. The N_2H_2 and N_2H_4 ligands bridge two enantiomeric [Ru(PPh_3)('tpS_4')] fragments, and the centers of the N–N bonds represent the inversion centers. The average Ru–S distances in the hydrazine complex **18**·4THF (235.1 pm) and the diazene complex **19**·4CH_2Cl_2 (236.6 pm) are also similar. The difference of 1.5 pm is a result of different Ru–S2 distances *trans* to the N_2H_4 and N_2H_2 ligands, which are 227.5(4) pm (**18**·4THF) vs. 232.9(2) pm (**19**·4CH_2Cl_2). All other Ru–S distances are identical within the 3σ criterion in both **18**·4THF and **19**·4CH_2Cl_2.

The Ru–S2 distance of **19**·4CH_2Cl_2 [232.9(2) pm] indicates the *trans* bond lengthening influence of the σ-π ligand N_2H_2, since the corresponding Ru–S2 distances of the σ ligand N_2H_4 and pyridine complexes **18**·4THF [227.5(4) pm] and **7** [227.7(1) pm] are shorter. The Ru–S distances *trans* to N_2H_2 in the closely related complexes [μ-N_2H_2{Ru(PPh_3)('S_4')$}_2$] [228.2(2) pm] and [μ-N_2H_2{Ru(PPh_3)('$^{bu}S_4$')$}_2$] [230.7(3) pm][12] are slightly shorter than in **19**·4CH_2Cl_2. Nonetheless, as in **19**·4CH_2Cl_2, the Ru–S bonds *trans* to the N_2H_2 ligand always represent the shortest Ru–S bonds in [μ-N_2H_2{RuS_4}$_2$] complexes so far characterized.

The different bonding properties of N_2H_2 and N_2H_4 are also illustrated by the Ru–N distances of **18**·4THF [214.4(9) pm] and **19**·4CH_2Cl_2 [203.0(7) pm], indicating Ru–N single and partial Ru–N double bonds. The Ru–N distance in **18**·4THF is comparable with that of the pyridine complex **7** [215.5(3) pm], while the Ru–N distance in **19**·4CH_2Cl_2 is rationalized by the [M=NH=NH=M] 4c-6e$^-$ π bonding system, which is characteristic of this type of [μ-N_2H_2{M}$_2$] complex.[12] The N–N distances in **18**·4THF [149(2) pm] and in **19**·4CH_2Cl_2 [129(1) pm] correspond with N–N single and slightly elongated N–N double bonds.

In both **18**·4THF and **19**·4CH_2Cl_2, the Ru centers and the thiolate donors form approximated planes. When least-squares planes are calculated through the six atoms Ru1, S1, S4, Ru1A, S1A, and S4A, the largest deviations from these planes are observed for the Ru centers, being 11.0(2) pm (**18**·4THF) and 10.8(1) pm (**19**·4CH_2Cl_2), respectively. In the diazene complex **19**·4CH_2Cl_2, the diazene N atoms are also coplanar, deviating by only 5.5(6) pm. In the hydrazine complex **18**·4THF, the hydrazine N atoms show a large deviation of 25.9(9) pm from the respective plane. This deviation gives rise to a step-like arrangement of the two enantiomeric [Ru(NH_2)(PPh_3)('tpS_4')] halves of **18**·4THF. The step height, calculated as distance between the two least-squares planes [Ru1, S1, S2, S4, N1] and [Ru1A, S1A, S2A, S4A, N1A], is 52.8 pm. The step-like arrangement of the two [$RuNPS_4$] cores in **18**·4THF is also reflected by the [S4–Ru1–N1–N1A] torsion angle of –151.9(1)°. [In the diazene complex, in which the Ru, the thiolate S and diazene N atoms form a nearly perfect plane, the corresponding angle is 173.9(9)°, close to the ideal of 180°.]

The arrangement of Ru, thiolate S, diazene N, or hydrazine N atoms enables the formation of stabilizing N–H···S hydrogen bonds in both **18**·4THF and **19**·4CH_2Cl_2. The N–H···S bonds are indicated by both the N–H···S vectors and the distances, which are shorter than the sum of the corresponding van der Waals radii (r_H = 120 pm, r_S = 185 pm) (Figure 5).

In the diazene complex **19**·4CH_2Cl_2, two bifurcated and nearly planar N–H···S_2 (thiolate) bridges exist [*d*(H1···S1A) = 258 pm, *d*(H1···S4) = 289 pm]. In the hydrazine complex **18**·4THF, two similar but nonplanar bifurcated hydrogen bonds are indicated by the H1···S1A (258 pm) and H1···S4 (298 pm) distances. It is significant that in the hydrazine complex the H2···S3A and the corresponding H2A···S3 distances of 288 pm indicate two additional hydrogen bonds between the thioether S atoms S3 and S3A and the NH_2 group atoms H2, and H2A. (Assuming sp^3 hybridization of the thioether S donors, the lone pairs at S3 and S3A indeed point directly at the positions of H2 and H2A respectively.)

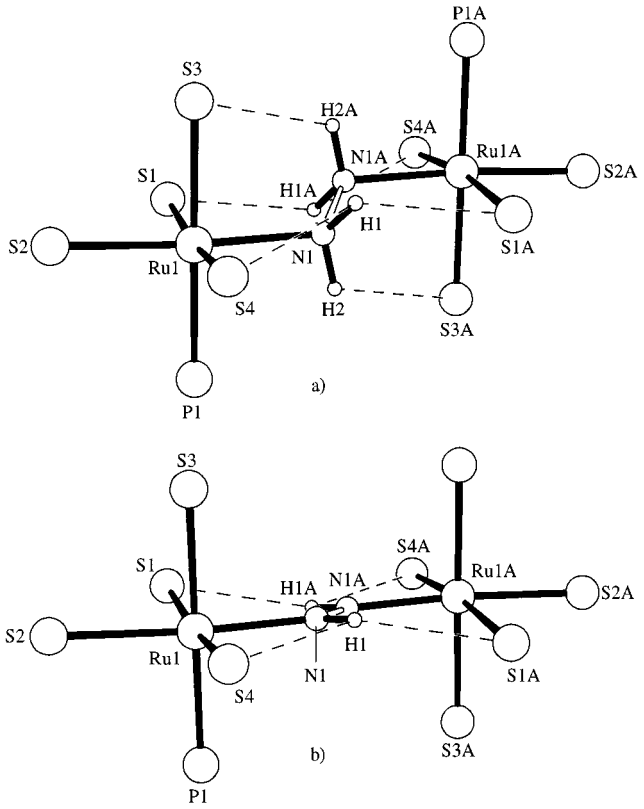

Figure 5. The [μ-N_2H_x{$RuPS_4$}$_2$] cores of a) **18**·4THF (x = 4) and b) **19**·4CH_2Cl_2 (x = 2) illustrating the [μ-N_2H_x{RuS_2(thiolate)}$_2$] planes and NH···S bridges

Due to the inversion center, the two NH_2 groups in **18**·4THF assume a staggered conformation, in contrast to the conformation in free hydrazine which exhibits a dihedral angle of about 95°.[16]

Discussion and Conclusion

The [Ru('tpS_4')] fragment exhibits a similarly versatile coordination chemistry as the [Ru('$^RS_4$')] fragments and binds a large number of coligands ranging from CO, NO, CR_2, PR_3 to N_3^-, N_2H_2, N_2H_4, and NH_3. In addition, [Ru('tpS_4')] complexes undergo reactions and yield species not yet observed with [Ru('$^RS_4$')] fragments. For example, [Ru(PPh_3)$_2$('tpS_4')] (**1**) exchanges both of its PPh_3 ligands with DMSO or PEt_3. When the [Ru(NO)(PPh_3)('tpS_4')]$^+$ (**13**) cation is reduced to give the neutral 19 valence electron species [Ru(NO)(PPh_3)('tpS_4')] (**14**), the 'tpS_4'$^{2-}$ ligand stays intact, in contrast to the '$^RS_4$'$^{2-}$ ligands, which undergo C–S cleavage reactions.[6]

In the search for labile [Ru('tpS_4')] precursor complexes, [Ru(PPh_3)$_2$('tpS_4')] (**1**) was found to exclusively exchange one PPh_3 for nitrogenous ligands. This enabled the synthesis of N_2H_4 and NH_3 complexes and, in particular, of the acetonitrile complex [Ru(MeCN)(PPh_3)('tpS_4')] (**12**). Complex **12** made feasible the synthesis of the azido, iodo, and nitrosyl complexes. All attempts to obtain dinitrogen complexes have so far remained unsuccessful also with the [Ru('tpS_4')] fragment. However, structurally characterized transition metal sulfur complexes containing the hydrazine and diazene couple could be obtained for the first time. The complexes [μ-N_2H_4{Ru(PPh_3)('tpS_4')}$_2$] (**18**) and [μ-N_2H_2{Ru(PPh_3)('tpS_4')}$_2$] (**19**) permitted a detailed analysis of the structural and bonding properties of hydrazine versus diazene complexes. The structural parameters indicate bifurcated N–H···S_2(thiolate) hydrogen bonds in both **18** and **19** and additional N–H···S(thioether) bridges in the hydrazine complex **18**. The increased number of N–H···S hydrogen bonds formed when going from the diazene to hydrazine complexes is significant with regard to the "open-side" model of the FeMoco function in nitrogenases.[4a], [13a] According to this model, N_2 is activated through binding to two low-spin Fe^{II} centers in [S, N, O] coordination spheres. Over the course of three subsequent [2 H^+, 2 e^-] reduction steps yielding NH_3 via N_2H_2 and N_2H_4 intermediates, an increased number of N–H···S(O) hydrogen bonds is instrumental in keeping the redox potential in the range –280 mV to ca. –500 mV, which are the both the thermodynamic limiting and biologically compatible values of enzymatic N_2 reduction.

Experimental Section

General Methods: Unless otherwise noted, all reactions and operations were carried out at room temperature under nitrogen using standard Schlenk techniques. Solvents were dried and distilled before use. As far as possible, reactions were monitored by IR or NMR spectroscopy. – Spectra were recorded with the following instruments: IR (KBr disks or CaF_2 cuvettes, solvent bands were compensated): Perkin–Elmer 983, 1620 FT IR, and 16PC FT-IR. – NMR: Jeol FT-JNM-GX 270, EX 270, and Lambda LA 400 with the protio solvent signals used as a reference. Chemical shifts are quoted on the δ scale (downfield shifts are positive) relative to tetramethylsilane (^{1}H, ^{13}C{^{1}H} NMR) or 85% H_3PO_4 (^{31}P{^{1}H} NMR). Spectra were recorded at 25 °C. – Mass spectra: Jeol MSTATION 700 spectrometer. – UV/Vis: Shimadzu UV-3101 – Elemental analysis: Carlo Erba EA 1106 or 1108 analyzer. – Cyclic voltammetry was performed with a PAR 264A potentiostat using a three-electrode cell with glassy carbon ROTEL A working, Pt reference and Pt counter electrodes. Solutions were 10^{-3} M in complex. TBA[PF_6] (10^{-1} M) was used as conducting electrolyte. Potentials were referenced to the normal hydrogen electrode via Fc/Fc$^+$ as internal standard (E_{Fc/Fc^+} = +0.4 V versus normal hydrogen electrode).[17] – $N_2C(CO_2Et_2)_2$,[18] $K_2C_2N_2O_4$,[19] [$RuCl_2$-$(DMSO)_4$],[20] [$RuCl_2(PMe_3)_4$],[21] NEt_4N_3,[22] [Ru(PPh_3)$_2$-('tpS_4')] (**1**),[7] and 'tpS_4'–H_2,[7] were prepared as described in the literature, LiOMe, MeI, $NOBF_4$, $LiBEt_3H$, NH_2NHMe, and N_2H_4 were purchased from Aldrich.

[Ru(PEt_3)$_2$('tpS_4')] (2): PEt_3 (0.5 mL, 3.4 mmol) was added to a yellow-orange suspension of [Ru(PPh_3)$_2$('tpS_4')] (**1**) (190 mg, 0.19 mmol) in THF (10 mL) and heated at reflux for 3 min. The resultant yellow solution was cooled to room temperature, and concentrated to dryness. The yellow residue was dissolved in THF (5 mL), the resulting solution was filtered, layered with *n*-hexane (50 mL) and cooled to –30 °C. Yellow microcrystals precipitated, which were separated after 1 d, washed with *n*-hexane (40 mL) and dried in vacuo. Yield: 70 mg of **2**·0.5THF (50%). – $C_{32}H_{46}O_{0.5}P_2RuS_4$ (**2**·0.5THF) (730.0): calcd. C 52.65, H 6.35, S

17.57; found C 52.90, H 6.56, S 17.21. – MS (FD, CH_2Cl_2, ^{102}Ru); *m/z*: 694 [Ru(PEt_3)$_2$('tpS_4')]$^+$. – ^1H NMR (CD_2Cl_2, 269.6 MHz): δ = 7.95–7.85 (m, 2 H, C_6H_4), 7.75 (d, 2 H, C_6H_4), 7.35 (d, 2 H, C_6H_4), 7.25–7.18 (m, 2 H, C_6H_4), 6.90–6.75 (m, 4 H, C_6H_4), 1.95–1.75 (m, 12 H, P–CH_2CH$_3$), 1.10–0.97 (m, 15 H, P–CH$_2$CH_3). – $^{13}C\{^1H\}$ NMR (100.40 MHz, CD_2Cl_2): δ = 158.9, 138.6, 136.8, 132.0, 131.5, 130.2, 129.7, 128.8, 121.1 [*C*(aryl)], 19.2 (t, P–*C*H$_2$CH$_3$), 8.5 (P–CH$_2$*C*H$_3$). – $^{31}P\{^1H\}$ NMR (109.38 MHz, CD_2Cl_2): δ = 18.0 (s).

[Ru(DMSO)$_2$('tpS$_4$')] (3): A yellow-orange suspension of [Ru(PPh_3)$_2$('tpS_4')] (**1**) (196 mg, 0.20 mmol) in DMSO (15 mL) was heated at reflux for 5 min, yielding a yellow-green solution. The solution was cooled to room temperature, combined with MeOH (75 mL), and stirred for 12 h. A yellow solid precipitated, which was separated, washed with MeOH (30 mL), Et_2O (20 mL), and dried in vacuo. Despite several recrystallizations from CH_2Cl_2/MeOH, satisfactory elemental analyses could not be obtained. However, the NMR spectra of the yellow solid showed the absence of any PPh_3 resulting from the precursor complex **1**. Yield: 50 mg of **3** (41%). – $C_{22}H_{24}O_2RuS_6$ (**3**) (613.9): calcd. C 43.05, H 3.94; found C 44.42, H 4.13. – IR (KBr): $\tilde{\nu}$ = 1015 cm^{-1}, s, ν(SO). – MS (FD, CH_2Cl_2, ^{102}Ru); *m/z*: 614 [Ru(DMSO)$_2$('tpS_4')]$^+$. – ^1H NMR (269.6 MHz, CD_2Cl_2): δ = 7.85–7.80 (m, 2 H, C_6H_4), 7.65 (d, 2 H, C_6H_4), 7.50 (d, 2 H, C_6H_4), 7.33–7.28 (m, 2 H, C_6H_4), 7.00 (t, 2 H, C_6H_4), 6.87 (t, 2 H, C_6H_4), 3.25 (s, 3 H, S–CH_3), 3.05 (s, 3 H, S–CH_3). – $^{13}C\{^1H\}$ NMR (100.40 MHz, CD_2Cl_2): δ = 153.9, 137.1, 136.9, 132.5, 131.8, 130.7, 130.6, 130.0, 122.8, (C_6H_4), 46.3, 44.9 (S–*C*H$_3$).

[Ru(I)(PPh$_3$)('tpS$_4$–Me$_2$')]I (4): MeI (0.5 mL, 8.0 mmol) was added while stirring to a yellow-orange solution of [Ru(PPh_3)$_2$('tpS_4')] (**1**) (140 mg, 0.14 mmol) in CH_2Cl_2 (30 mL) which changed its color to yellow over the course of 2 h. After addition of *n*-hexane (40 mL), a yellow solid precipitated, which was separated, washed with MeOH (10 mL), *n*-hexane (20 mL), and dried in vacuo. Recrystallization from CH_2Cl_2/Et_2O (20 mL/ 40 mL) yielded yellow crystals, which were separated, washed with Et_2O (20 mL), and dried in vacuo. Yield: 100 mg of **4** (71%). – $C_{38}H_{33}I_2PRuS_4$ (**4**) (1004): calcd. C 45.47, H 3.31, S 12.78; found C 45.25, H 3.50, S 12.59. – ^1H NMR (CD_2Cl_2, 269.6 MHz): δ = 8.30 (t, 2 H, C_6H_4), 8.00 (d, 1 H, C_6H_4), 7.90–7.80 (m, 1 H, C_6H_4), 7.75–7.60 [m, 8 H, C_6H_4 and P(C_6H_5)$_3$], 7.60–7.30 [m, 15 H, C_6H_4 and P(C_6H_5)$_3$], 2.85 (s, 3 H, S–CH_3), 2.05 (s, 3 H, S–CH_3). – $^{31}P\{^1H\}$ NMR (109.38 MHz, CD_2Cl_2): δ = 23.5 (s).

[Ru(PMe$_3$)(PPh$_3$)('tpS$_4$')] (5): PMe_3 (0.8 mL, 7.70 mmol) was added to a yellow suspension of [Ru(PPh_3)$_2$('tpS_4')] (**1**) (400 mg, 0.41 mmol) in THF (15 mL). The suspension was stirred for 3 h, during the course of which a yellow solution resulted, which was filtered and concentrated to dryness to give a yellow residue. The residue was digested with *n*-hexane (40 mL) for 1 h, separated, washed with *n*-hexane (40 mL), and dried in vacuo. Yield 180 mg of **5** (55%). – $C_{39}H_{36}P_2RuS_4$ (**5**) (796.0): calcd. C 58.85, H 4.56, S 16.11; found C 59.10, H 4.57, S 15.52. – IR (KBr): $\tilde{\nu}$ = 953 cm^{-1}, δ(PCH). – MS (FD, CH_2Cl_2, ^{102} Ru); *m/z*: 796 [Ru(PMe_3)(PPh_3)('tpS_4')]$^+$. – ^1H NMR (269.6 MHz, CD_2Cl_2): δ = 7.86–7.74 (m, 3 H, C_6H_4), 7.59–7.46 [m, 7 H, C_6H_4 and P(C_6H_5)$_3$], 7.26–7.23 [m, 11 H, C_6H_4 and P(C_6H_5)$_3$], 7.09 (d, 1 H, C_6H_4), 6.96–6.94 (m, 2 H, C_6H_4), 6.85 (t, 1 H, C_6H_4), 6.65 (t, 1 H, C_6H_4), 6.56 (t, 1 H, C_6H_4), 1.16 [d, *J* = 4.32 Hz, 9 H, P(CH_3)]. – $^{13}C\{^1H\}$ NMR (67.8 MHz, CD_2Cl_2): δ = 159.0 (d, J_{PC} = 5.96 Hz), 156.2 (d, J_{PC} = 7.95 Hz), 138.9, 138.7, 138.2, 138.0, 136.6, 136.1, 135.9, 135.3, 134.6 (d, J_{PC} = 9.93 Hz), 132.2, 131.4, 130.5, 129.8 (d, J_{PC} = 3.48 Hz), 129.7, 129.5, 129.2, 128.5, 127.4 (d, J_{PC} = 8.94 Hz), 121.2, 121.1 [*C*(aryl)], 18.3 [d, J_{PC} = 9.94 Hz, (P(*C*H$_3$)], 17.9 [d, J_{PC} = 9.94, (P(*C*H$_3$)]. – $^{31}P\{^1H\}$ NMR (109.38 MHz, CD_2Cl_2): δ = –6.5 (d, *P*Me$_3$), +37 (d, *P*Ph$_3$).

[Ru(PMe$_3$)$_2$('tpS$_4$')] (6): Solid Li_2–'tpS_4' (159 mg, 0.43 mmol) was added to a stirred suspension of [RuCl_2(PMe_3)$_4$] (205 mg, 0.43 mmol) in MeOH (10 mL), which was heated at reflux for 4 h, yielding a yellow solution from which yellow microcrystals started precipitating. Cooling to room temperature completed the precipitation. The resulting yellow microcrystals were separated, washed with MeOH (15 mL) and *n*-hexane (20 mL), and dried in vacuo. Yield: 120 mg of **6** (46%). – $C_{24}H_{30}P_2RuS_4$ (**6**) (609.8): calcd. C 47.27, H 4.96, S 21.03; found C 47.20, H 4.88, S 21.11. – IR (KBr, cm^{-1}): $\tilde{\nu}$ = 958, 943 vs, δ(PCH). – MS (FD, CH_2Cl_2, ^{102}Ru); *m/z*: 610 [Ru(PMe_3)$_2$('tpS_4')]$^+$. – ^1H NMR ([D$_8$]THF, 399.65 MHz): δ = 7.97–7.93 (m, 2 H, C_6H_4), 7.77 (d, 2 H, C_6H_4), 7.29 (d, 2 H, C_6H_4), 7.20–7.16 (m, 2 H, C_6H_4), 6.80–6.76 (m, 2 H, C_6H_4), 6.72–6.68 (m, 2 H, C_6H_4), 1.41 (d, *J* = 4.28 Hz, 18 H, P–CH_3). – $^{13}C\{^1H\}$ NMR (100.40 MHz, [D$_8$]THF): δ = 159.8 (t), 139.7 (t), 137.3, 132.7–132.5 (m), 132.5, 130.9, 130.0, 128.8, 121.0 [*C*(aryl)], 18.9–18.0 (m, P–*C*H$_3$). – $^{31}P\{^1H\}$ NMR (161.70 MHz, [D$_8$]THF): δ = 7.7 (s).

[Ru(py)(PPh$_3$)('tpS$_4$')] (7): A yellow-orange suspension of [Ru(PPh_3)$_2$('tpS_4')] (**1**) (235 mg, 0.24 mmol) in pyridine (7 mL) was heated at reflux for 10 min to give an orange-red solution. The solution was cooled to room temperature, combined with MeOH (70 mL), and stirred for 1 h. A yellow solid precipitated, which was separated, washed with MeOH (40 mL) and Et_2O (40 mL), and dried in vacuo. Yield 125 mg of **7** (65%). – $C_{41}H_{32}NPRuS_4$ (**7**) (799.0): calcd. C 61.63, H 4.04, N 1.75, S 16.05; found C 61.41, H 3.89, N 1.99, S 16.15. – MS (FD,CH_2Cl_2, ^{102}Ru); *m/z*: 799 [Ru(py)(PPh_3)('tpS_4')]$^+$. – ^1H NMR (269.6 MHz, CD_2Cl_2): δ = 8.50 [d, 2 H, *o*-*H*(py)], 7.95 (d, 1 H, C_6H_4), 7.70 (d, 1 H, C_6H_4), 7.65–7.60 (m, 1 H, C_6H_4), 7.53–7.48 (m, 1 H, C_6H_4), 7.40–7.30 [m, 6 H, C_6H_4 and P(C_6H_5)$_3$], 7.25–7.10 [m, 12 H, C_6H_4, P(C_6H_5)$_3$ and py], 7.05–6.90 (m, 3 H, C_6H_4), 6.80–6.75 (m, 3 H, C_6H_4), 6.65 (t, 1 H, C_6H_4), 6.55 (t, 1 H, C_6H_4). – $^{31}P\{^1H\}$ NMR (109.38 MHz, CD_2Cl_2): δ = 41.50 (s).

[Ru(NH$_3$)(PPh$_3$)('tpS$_4$')] (8): NH_3 gas was bubbled through a refluxing yellow-orange suspension of [Ru(PPh_3)$_2$('tpS_4')] (**1**) (200 mg, 0.20 mmol) in THF (25 mL) for 5 min. A yellow-orange solution resulted which was cooled to room temperature, combined with *n*-hexane (100 mL), and stirred for 2 h. A yellow solid precipitated, which was separated, washed with *n*-hexane (40 mL), and dried in vacuo. Yield 100 mg of **8**·THF (65%). – $C_{38}H_{34}NO_{0.5}PRuS_4$ (**8**·0.5THF) (773.0): calcd. C 59.04, H 4.43, N 1.81, S 16.59; found C 59.03, H 4.21, N 1.67, S 16.33. – IR (KBr, cm^{-1}): $\tilde{\nu}$ = 3348, 3245, ν(NH). – ^1H NMR (399.65 MHz, CD_2Cl_2) δ = 7.95 (d, 1 H, C_6H_4), 7.86 (d, 2 H, C_6H_4), 7.69–7.64 [m, 6 H, C_6H_4 and P(C_6H_5)$_3$], 7.46 (d, 1 H, C_6H_4), 7.36–7.26 [m, 12 H, C_6H_4 and P(C_6H_5)$_3$], 6.97 (t, 1 H, C_6H_4), 6.90–6.86 (m, 2 H, C_6H_4), 6.57–6.52 (m, 2 H, C_6H_4), 1.70 (s, 3 H, NH_3). – $^{31}P\{^1H\}$ NMR (109.38 MHz, CD_2Cl_2): δ = 47.5 (s).

[Ru(N$_2$H$_4$)(PPh$_3$)('tpS$_4$')] (9): N_2H_4 (0.25 mL, 8.00 mmol) was added to a stirred yellow-orange suspension of [Ru(PPh_3)$_2$('tpS_4')] (**1**) (250 mg, 0.25 mmol) in THF (20 mL), which was heated at reflux for 10 min to give a yellow-orange solution. The solution was cooled to room temperature, filtered, combined with *n*-hexane (80 mL), and stirred for 1 h. A yellow solid precipitated, which was separated, washed with MeOH (10 mL) and *n*-hexane (40 mL), and dried in vacuo. Yield: 100 mg of **9** (53%). – $C_{36}H_{31}N_2PRuS_4$ (**9**) (752.0): calcd. C 57.50, H 4.16, N 3.73, S 17.06; found C 56.74, H 4.37, N 3.64, S 16.86. – IR (KBr, cm^{-1}): $\tilde{\nu}$ = 3334, 3292, 3245, 3164

ν(NH). – MS (FD, CH_2Cl_2, ^{102}Ru); *m/z*: 749 [Ru(N$_2$H)(PPh_3)('tpS_4')]$^+$. – ^{1}H NMR (269.6 MHz, CD_2Cl_2): δ = 7.95 (d, 1 H, C_6H_4), 7.85–7.77 (m, 2 H, C_6H_4), 7.65–7.59 [m, 6 H, C_6H_4 and $P(C_6H_5)_3$], 7.47 (d, 1 H, C_6H_4), 7.27–7.22 [m, 12 H, C_6H_4 and $P(C_6H_5)_3$], 7.98–6.82 (m, 3 H, C_6H_4), 6.53–6.50 (m, 2 H, C_6H_4), 4.20 (m, 1 H, NH_2), 4.09 (m, 2 H, NH_2), 3.36 (s, 1 H, NH_2). – $^{31}P\{^1H\}$ NMR (109.38 MHz, CD_2Cl_2): δ = 44.0 (s).

[Ru(N$_2$H$_3$Me)(PPh_3)('tpS_4')] (10): N_2H_3Me (0.52 mL, 10.0 mmol) was added to a yellow-orange suspension of [Ru(PPh_3)$_2$('tpS_4')] (**1**) (200 mg, 0.20 mmol) in THF (10 mL). The suspension was heated at reflux for 45 min, during the course of which a yellow-orange solution resulted. The solution was cooled to room temperature, filtered, and combined with *n*-hexane (80 mL). A yellow solid precipitated, which was separated, washed with MeOH (10 mL), *n*-hexane (20 mL), and dried in vacuo. Yield: 105 mg of **10** (69%). – $C_{37}H_{33}N_2PRuS_4$ (**10**) (766.0): calcd. C 58.02, H 4.34, N 3.66, S 16.74; found C 57.06, H 4.43, N 3.67, S 16.38. – ^{1}H NMR (269.6 MHz, CD_2Cl_2): δ = 7.95 (d, 1 H, C_6H_4), 7.84 (d, 1 H, C_6H_4), 7.79–7.75 (m, 1 H, C_6H_4), 7.67–7.61 [m, 6 H, C_6H_4 and $P(C_6H_5)_3$], 7.45 (d, 1 H, C_6H_4), 7.28–7.20 [m, 12 H, C_6H_4 and $P(C_6H_5)_3$], 6.95–6.80 (m, 3 H, C_6H_4), 6.54–6.48 (m, 2 H, C_6H_4), 3.97 (t, *J* = 4.16 Hz, 1 H, NH_2), 3.84–3.81 (m, 1 H, NH_2), 3.38–3.29 (m, 1 H, NH_2), 2.09 (d, *J* = 6.88 Hz, 3 H, CH_3). – $^{13}C\{^1H\}$ NMR (67.8 MHz, CD_2Cl_2): δ = 156.7 (d, J_{PC} = 6.22 Hz), 153.1, 142.3, 142.2, 139.0, 135.9, 135.8, 134.1 (d, J_{PC} = 9.84 Hz), 133.5, 132.9, 132.3, 131.7 (d, J_{PC} = 5.17 Hz), 131.2, 130.7, 130.2, 129.8, 129.6, 129.3, 128.4, 128.0 (d, J_{PC} = 9.32 Hz), 121.8, 120.9 [*C*(aryl)], 42.8 (*C*H$_3$). – $^{31}P\{^1H\}$ NMR (109.38 MHz, CD_2Cl_2): δ = 47.0 (s).

[Ru{C(CO$_2$Et)$_2$}(PPh_3)('tpS_4')] (11): $N_2C(CO_2Et)_2$ (0.5 mL, 3.10 mmol) was added to a yellow-orange suspension of [Ru(PPh_3)$_2$('tpS_4')] (**1**) (200 mg, 0.20 mmol) in THF (15 mL). The suspension was heated at reflux for 4 h, over the course of which a yellow-orange solution resulted. The solution was cooled to room temperature, filtered, and combined with *n*-hexane (40 mL). A yellow solid precipitated, which was separated, washed with *n*-hexane (20 mL), and dried in vacuo. Yield: 100 mg of **11** (57%). – $C_{43}H_{37}O_4PRuS_4$ (**11**) (878.1): calcd. C 58.82, H 4.25, N 0.00, S 14.61; found C 58.76, H 4.21, N 0.41, S 13.90. – IR (KBr, cm^{-1}): $\tilde{\nu}$ = 1674, 1640 ν(CO). – MS (FD, CH_2Cl_2, ^{102}Ru); *m/z*: 878 [Ru{C(CO$_2$Et)$_2$}('tpS_4')]$^+$. – ^{1}H NMR (269.6 MHz, CD_2Cl_2): δ = 8.06–8.03 (m 1 H, C_6H_4), 7.94 (d, 2 H, C_6H_4), 7.71–7.65 [m, 5 H, C_6H_4 and $P(C_6H_5)_3$], 7.58 (d, 1 H, C_6H_4), 7.49 (t, 1 H, C_6H_4), 7.33–7.16 [m, 14 H, C_6H_4 and $P(C_6H_5)_3$], 6.86 (d, 1 H, C_6H_4), 6.67 (t, 1 H, C_6H_4), 6.40 (t, 1 H, C_6H_4), 4.30–4.14 (m, 1 H, COOCH_2CH$_3$), 4.03–3.83 (m, 2 H, COOCH_2CH$_3$), 3.76–3.64 (m, 1 H, COOCH_2CH$_3$), 1.16 (t, *J* = 3.58 Hz, 3 H, COOCH$_2$CH_3), 1.06 (t, *J* = 3.47 Hz, 3 H, COOCH$_2$CH_3). – $^{31}P\{^1H\}$ NMR (109.38 MHz, CD_2Cl_2): δ = 31.0 (s).

[Ru(MeCN)(PPh_3)('tpS_4')] (12): A yellow-orange suspension of [Ru(PPh_3)$_2$('tpS_4')] (275 mg, 0.28 mmol) in acetonitrile (35 mL) was heated at reflux for 3 h, yielding a yellow-orange solution. The solution was cooled to room temperature, filtered, concentrated in volume to 20 mL, combined with MeOH (50 mL), and stirred for 1 h. A yellow solid precipitated, which was separated, washed with MeOH (20 mL), Et_2O (40 mL), and dried in vacuo. Yield 150 mg of **12** (70%). – $C_{38}H_{30}NPRuS_4$ (**12**) (761.0): calcd. C 59.98, H 3.97, N 1.84, S 16.85; found C 59.87, H 4.09, N 2.01, S 16.69. – IR (KBr, cm^{-1}): $\tilde{\nu}$ = 2271 ν(CN). – MS (FD, CH_2Cl_2, ^{102}Ru); *m/z*: 720 [Ru(PPh_3)('tpS_4')]$^+$. – ^{1}H NMR (CD_2Cl_2, 269.6 MHz): δ = 7.95 (d, 1 H, C_6H_4), 7.80 (d, 1 H, C_6H_4), 7.70–7.60 [m, 7 H, C_6H_4 and $P(C_6H_5)_3$], 7.45–7.40 (m, 1 H, C_6H_4), 7.30–7.20 [m, 10 H, C_6H_4 and $P(C_6H_5)_3$], 7.15–7.05 (m, 2 H, C_6H_4), 6.95–6.80 (m, 3 H, C_6H_4), 6.55–6.45(m, 2 H, C_6H_4), 1.75 (s, 3 H, CH_3). – $^{31}P\{^1H\}$ NMR (109.38 MHz, CD_2Cl_2): δ = 42.5 (s).

[Ru(NO)(PPh_3)('tpS_4')]BF_4 (13): Solid $NOBF_4$ (29 mg, 0.25 mmol) was added to a stirred solution of [Ru(MeCN)(PPh_3)('tpS_4')] (**12**) (190 mg, 0.25 mmol) in CH_2Cl_2 (15 mL), whose color changed from yellow to red over the course of 3 h. Undissolved material was removed by filtration, and Et_2O (80 mL) was added dropwise to the filtrate. A red-brown solid precipitated, which was separated, washed with Et_2O (20 mL), and dried in vacuo. Yield: 85 mg of **13**·0.25CH_2Cl_2 (40%). – $C_{36.25}H_{27.5}BCl_{0.5}F_4NOPRuS_4$ (**13**·0.25CH_2Cl_2) (858.0): calcd. C 50.75, H 3.23, N 1.63, S 14.95; found C 50.74, H 3.41, N 1.62, S 14.80. – IR (KBr, cm^{-1}): $\tilde{\nu}$ = 1852 ν(NO). – MS (FD, CH_2Cl_2, ^{102}Ru); *m/z*: 750 [Ru(NO)(PPh_3)$_2$('tpS_4')]$^+$. – ^{1}H NMR (CD_2Cl_2, 269.6 MHz): δ = 8.13 (d, 1 H, C_6H_4), 7.90 (d, 1 H, C_6H_4), 7.67–7.47 [m, 18 H, C_6H_4 and $P(C_6H_5)_3$], 7.43–7.40 (m, 1 H, C_6H_4), 7.31–7.11 (m, 3 H, C_6H_4), 7.00–6.96 (m, 2 H, C_6H_4), 6.88–6.81 (m, 1 H, C_6H_4). – $^{13}C\{^1H\}$ NMR (100.40 MHz, CD_2Cl_2): δ = 151.3 (d), 150.2, 134.5, 134.3, 133.7, 133.3, 133.3, 133.2, 133.0, 132.9, 132.0, 131.7, 131.5, 131.2, 129.9, 129.6, 129.5, 129.2, 126.7, 126.3, 125.7, 125.5 [*C*(aryl)]. – $^{31}P\{^1H\}$ NMR (109.38 MHz, CD_2Cl_2): δ = 25.0 (s).

[Ru(NO)(PPh_3)('tpS_4')] (14): NO gas was bubbled through a yellow solution of [Ru(MeCN)(PPh_3)('tpS_4')] (**12**) (210 mg, 0.28 mmol) in CH_2Cl_2 (20 mL) for 1 min. A deep-red solution resulted, which was stirred for 20 h. After addition of *n*-hexane (30 mL) a red-brown solid precipated, which was separated, washed with *n*-hexane (20 mL), and dried in vacuo. Yield 70 mg of **14** (34%). – $C_{36}H_{27}NOPRuS_4$ (**14**) (749.9): calcd. C 57.66, H 3.63, N 1.87, S 17.10; found C 55.03, H 3.67, N 2.04, S 17.18. – IR (KBr, cm^{-1}): $\tilde{\nu}$ = 1598 ν(NO). – MS (FD, CH_2Cl_2, ^{102}Ru); *m/z*: 750 [Ru(NO)(PPh_3)$_2$('tpS_4')]$^+$.

(NEt$_4$)[Ru(N$_3$)(PPh_3)('tpS_4')] (15): NEt_4N_3 (50 mg, 0.29 mmol) was added to a yellow suspension of [Ru(MeCN)(PPh_3)('tpS_4')] (**12**) (220 mg, 0.29 mmol) in acetone (20 mL). Under exclusion of light, the mixture was stirred for 3 h during which time an orange solution resulted. Addition of Et_2O (80 mL) to the solution yielded an orange solid, which was separated after 1 h, washed with Et_2O (40 mL) and dried in vacuo. Yield: 146 mg of **15** (56%). – $C_{44}H_{47}N_4PRuS_4$ (**15**) (892.2): calcd. 59.24, H 5.31, N 6.28, S 14.37; found C 58.07, H 5.47, N 5.81, S 15.10. – IR (KBr, cm^{-1}): $\tilde{\nu}$ = 2029 ν(N$_3$). – ^{1}H NMR ([D$_6$]acetone, 269.6 MHz): δ = 8.87 (d, 1 H, C_6H_4), 8.73–8.68 (m, 1 H, C_6H_4), 8.58–8.53 [m, 6 H, C_6H_4 and $P(C_6H_5)_3$], 8.43 (d, 1 H, C_6H_4), 8.00–7.90 [m, 13 H, C_6H_4 and $P(C_6H_5)_3$], 7.79 (d, 1 H, C_6H_4), 7.68–7.58 (m, 2 H, C_6H_4), 7.33–7.27 (m, 1 H, C_6H_4), 7.15–7.10 (m, 1 H, C_6H_4), 4.15 (q, *J* = 3.71 Hz, 8 H, N–CH_2), 2.10–2.05 (m, 12 H, N–CH$_2$–CH_3).

[Ru(I)(PPh_3)('tpS_4')] (16): Elemental iodine (40 mg, 0.16 mmol) was added to a stirred suspension of [Ru(MeCN)(PPh_3)('tpS_4')] (**12**) (240 mg, 0.31 mmol) in THF (15 mL). Over the course of 5 min a clear red solution resulted from which dark red microcrystals crystallized. The crystals were separated after 12 h, washed with THF (20 mL), Et_2O (20 mL), and dried in vacuo. Yield: 200 mg of **16**·THF (70%). – $C_{40}H_{35}IOPRuS_4$ (**16**·THF) (918.9): calcd. C 52.28, H 3.84, S 13.96; found C 52.43, H 3.92, S 13.80. – MS (FD, CH_2Cl_2, ^{102}Ru); *m/z*: 847 [Ru(I)(PPh_3)$_2$('tpS_4')]$^+$.

[Ru(N$_3$)(PPh_3)('tpS_4')] (17): NEt_4N_3 (67 mg, 0.39 mmol) was added to a stirred suspension of [Ru(I)(PPh_3)('tpS_4')]·THF (**16**) (165 mg, 0.18 mmol) in acetone (15 mL). Under exclusion of light, the suspension was stirred for 2.5 d during which time its color changed to yellow-green. The yellow-green solid was separated, washed with MeOH (40 mL), acetone (40 mL) and Et_2O (20 mL), and dried in

Table 2. Selected crystallographic data of [Ru(py)(PPh$_3$)('tpS$_4$')] (**7**), [Ru(NO)(PPh$_3$)('tpS$_4$')]BF$_4$·CH$_2$Cl$_2$ (**13**·CH$_2$Cl$_2$), [Ru(I)(PPh$_3$)-('tpS$_4$')]·CH$_2$Cl$_2$ (**16**·CH$_2$Cl$_2$), [μ-N$_2$H$_4${Ru(PPh$_3$)('tpS$_4$')}$_2$]·4THF (**18**·4THF), and [μ-N$_2$H$_2${Ru(PPh$_3$)('tpS$_4$')}$_2$]·4CH$_2$Cl$_2$ (**19**·4CH$_2$Cl$_2$)

Compound	**7**	**13**·CH$_2$Cl$_2$	**16**·CH$_2$Cl$_2$	**18**·4THF	**19**·4CH$_2$Cl$_2$
Empirical formula	$C_{41}H_{32}NPRuS_4$	$C_{37}H_{29}BCl_2F_4NOPRuS_4$	$C_{37}H_{29}Cl_2IPRuS_4$	$C_{88}H_{90}N_2O_4P_2Ru_2S_8$	$C_{76}H_{64}Cl_8N_2P_2Ru_2S_8$
M_r [g/mol]	799.0	921.6	931.7	1760	1809
Crystal size [mm]	0.44 × 0.30 × 0.16	0.42 × 0.35 × 0.12	0.30 × 0.30 × 0.20	0.30 × 0.30 × 0.10	0.20 × 0.15 × 0.01
F(000)	816	928	1844	910	916
Crystal system	triclinic	triclinic	monoclinic	triclinic	triclinic
Space group	$P\bar{1}$	$P\bar{1}$	$P2_1/c$	$P\bar{1}$	$P\bar{1}$
a [pm]	984.0(2)	1037.6(1)	1094.0(1)	1034.8(4)	1102.96(4)
b [pm]	1007.9(1)	1205.9(1)	2452.8(3)	1451.7(4)	1334.71(5)
c [pm]	1794.4(3)	1676.2(2)	1369.0(1)	1479.3(6)	1545.90(5)
α [°]	88.76(1)	105.46(1)	90	115.90(2)	65.840(1)
β [°]	82.48(2)	96.00(1)	96.48(1)	91.90(2)	82.152(1)
γ [°]	77.12(1)	105.78(1)	90	93.68(3)	68.199(1)
V [nm^3]	1.7199(5)	1.9095(3)	3.6501(6)	1.990(1)	1.9276(1)
Z	2	2	4	1	1
$d_{calcd.}$ [g/cm^3]	1.543	1.603	1.695	1.469	1.559
μ [mm^{-1}]	0.778	0.863	1.721	0.683	0.972
Diffractometer	Siemens P4	Siemens P4	Siemens P4	Siemens P4	CCD (Bruker AXS)
Radiation [pm]	Mo-K_α (λ = 71.073)	Mo-K_α (λ = 71.073)	Mo-K_α (λ = 71.073)	Mo-K_α (λ = 71.073)	Mo-K_α (λ = 71.073)
Temperature [K]	200(2)	200(2)	200(2)	200(2)	210(2)
Scan technique	ω scan	ω scan	ω scan	ω scan	ω scan
2Θ range [°]	4.0–54.0	3.6–54.0	3.7–54.0	4.8–50.0	3.5–54.5
Scan speed [°/min]	4.0–40.0	4.0–40.0	5.0–50.0	8.0	–
Meas. reflections	8884	9579	9649	7698	10881
Indep. reflections	7497	8178	7956	6526	6557
R_{int} [%]	3.98	5.42	4.30	9.46	7.50
Obsd. reflections	5550	6189	6163	2795	3697
σ criterion	$F_o \geq 4\sigma(F)$	$F_o \geq 4\sigma(F)$	$F_o \geq 4\sigma(F)$	$F_o \geq 4\sigma(F)$	$F_o \geq 4\sigma(F)$
$R1$; $wR2$ [%]	4.33; 10.35	4.72; 10.79	4.22; 11.68	8.61; 16.49	7.26; 21.07
Ref. parameters	561	605	506	478	461

vacuo. Yield: 85 mg of **17**·0.5Me$_2$CO. – $C_{37.5}H_{30}N_3O_{0.5}PRuS_4$ (**17**·0.5Me$_2$CO) (791.0): calcd. C 56.94, H 3.82, N 5.31, S 16.22; found C 56.58, H 3.82, N 5.10, S 16.02. – IR (KBr, cm^{-1}): $\tilde{\nu}$ = 2036 ν (N_3). – MS (FD, CH$_2$Cl$_2$, ^{102}Ru); *m*/*z*: 762 [Ru(N_3)-(PPh$_3$)$_2$('tpS$_4$')]$^+$.

[μ-N$_2$H$_4${Ru(PPh$_3$)('tpS$_4$')}$_2$] (18): [Ru(N$_2$H$_4$)(PPh$_3$)('tpS$_4$')] (**9**) (120 mg, 0.16 mmol) was dissolved in CH$_2$Cl$_2$ (7 mL) and the solution was stirred for 7 d. After addition of MeOH (10 mL), yellow microcrystals precipitated, which were separated, washed with MeOH (10 mL), Et$_2$O (15 mL), and dried in vacuo. Yield: 20 mg of **17**·0.75CH$_2$Cl$_2$ (16%). – $C_{72.75}H_{59.5}Cl_{1.5}N_2P_2Ru_2S_8$ (**18**·0.75CH$_2$Cl$_2$) (1536): calcd. C 56.90, H 3.91, N 1.82, S 16.71; found C 56.72, H 4.03, N 2.01, S 16.30

[μ-N$_2$H$_2${Ru(PPh$_3$)('tpS$_4$')}$_2$] (19). – a) From [Ru(N$_2$H$_4$)-(PPh$_3$)('tpS$_4$')] (9) and O$_2$: [Ru(N$_2$H$_4$)(PPh$_3$)('tpS$_4$')] (**9**) (145 mg, 0.19 mmol) was dissolved in CH$_2$Cl$_2$ (20 mL) in a Schlenk tube that was closed by a septum. Air (20 mL, 0.19 mmol O$_2$) was injected into the solution by means of a syringe. Over the course of 36 h, the solution changed color from yellow to green, and green microcrystals precipitated. They were separated, washed with CH$_2$Cl$_2$ (5 mL), MeOH (15 mL), H$_2$O (10 mL) and Et$_2$O (20 mL), and dried in vacuo. Yield: 35 mg of **19**·CH$_2$Cl$_2$ (24%). – $C_{73}H_{58}Cl_2N_2P_2Ru_2S_8$ (**19**·CH$_2$Cl$_2$) (1555): calcd. C 56.40, H 3.76, N 1.80, S 16.50; found C 56.27, H 3.73, N 1.99, S 16.55. – UV/Vis (CH$_2$Cl$_2$): λ_{max} (nm) = 306.5 (ε = 15159 L mol^{-1} cm^{-1}), 463 (ε = 8162 L mol^{-1} cm^{-1}). – **b) From [Ru(MeCN)(PPh$_3$)('tpS$_4$')] (12), K$_2$N$_2$(CO$_2$)$_2$ and HAc:** 0.2 M acetic acid (3.45 mL, 0.69 mmol) was added dropwise to a stirred suspension of [Ru(-MeCN)(PPh$_3$)('tpS$_4$')] (**12**) (175 mg, 0.23 mmol) and K$_2$N$_2$(CO$_2$)$_2$ (134 mg, 0.69 mmol)in THF (25 mL). A dark green solution resulted with evolution of gas. Over the course of 5 min a green solid precipitated, which was separated after 3 h, washed with H$_2$O (15 mL), THF (25 mL), Et$_2$O (25 mL), and dried in vacuo. Yield: 153 mg of **19**·2H$_2$O (88%). – $C_{72}H_{60}N_2O_2P_2Ru_2S_8$ (**19**·2H$_2$O) (1506): calcd. C 57.43, H 4.02, N 1.86, S 17.03; found C 57.26, H 3.95, N 1.77, S 16.67.

X-ray Structure Analyses of [Ru(py)(PPh$_3$)('tpS$_4$')] (7), [Ru(NO)(PPh$_3$)('tpS$_4$')]BF$_4$·CH$_2$Cl$_2$ (13·CH$_2$Cl$_2$), [Ru(I)(PPh$_3$)-('tpS$_4$')]·CH$_2$Cl$_2$ (16·CH$_2$Cl$_2$), [μ-N$_2$H$_4${Ru(PPh$_3$)('tpS$_4$')}$_2$]·4THF (18·4THF), and [μ-N$_2$H$_2${Ru(PPh$_3$)('tpS$_4$')}$_2$]·4CH$_2$Cl$_2$ (19·4CH$_2$Cl$_2$): Orange crystals of **7** were grown by layering a hot pyridine solution of **7** with MeOH. Dark-brown platelets of **13**·CH$_2$Cl$_2$ formed when a saturated CH$_2$Cl$_2$ solution of **13** was layered with *n*-hexane. Black rhombohedra of [Ru(I)(PPh$_3$)('tpS$_4$')]·CH$_2$Cl$_2$ (**16**·CH$_2$Cl$_2$) were obtained when a saturated CH$_2$Cl$_2$ solution of **16** was layered with MeOH. Yellow platelets of [μ-N$_2$H$_4${Ru(PPh$_3$)('tpS$_4$')}$_2$]·4THF (**18**·4THF) crystallized from a THF solution of **18** layered with Et$_2$O. Green platelets of **19**·4CH$_2$Cl$_2$ formed when air was injected into a yellow solution of [Ru(N$_2$H$_4$)(PPh$_3$)('tpS$_4$')] (**9**) in CH$_2$Cl$_2$. – Suitable single crystals were mounted by using the oil-drop mounting technique.[23] For all data sets Lorentz and polarization corrections were applied. For **18**·4THF absorption effects have been neglected. A ψ-scan absorption correction has been applied for **7** (T_{min} = 0.4357, T_{max} = 0.4699), **13**·CH$_2$Cl$_2$ (T_{min} = 0.4254, T_{max} = 0.4680), and **16**·CH$_2$Cl$_2$ (T_{min} = 0.2677, T_{max} = 0.3412). An empirical correction was used for **19**·4CH$_2$Cl$_2$ (SADABS, T_{min} = 0.8294, T_{max} = 0.9923).[24] All structures were solved by direct methods and were refined using full-matrix least-squares procedures on F^2 (SHELXTL 5.03).[25] – All non-hydrogen atoms were refined anisotropically. The positions of the hydrogen atoms were taken from a difference Fourier map and were either refined isotropically (**7**), refined with a common isotropic displacement parameter (**13**·CH$_2$Cl$_2$ and **16**·CH$_2$Cl$_2$) or were kept fixed with a common isotropic displacement parameter

(**18**·4THF, **19**·4CH_2Cl_2). The BF_4 anion in the structure of **13**·CH_2Cl_2 is disordered around the B1-F11 vector, where two possible sites have been refined such that they are both equally occupied (50%). Furthermore, the solvate CH_2Cl_2 molecule is disordered with two different sites having occupancies of 74(4)% and 26(4)% respectively. In **16**·CH_2Cl_2, one Cl atom of the solvate molecule is disordered. Two possible sites have been refined with occupancies of 61(5)% and 39(5)%. In **19**·4CH_2Cl_2 two of the solvate molecules are disordered with site occupancies of the two possible sites being refined to 77(1)% and 29(1)%. The hydrogen atoms of the solvate molecules in all structures are geometrically positioned. Selected crystallographic data are summarized in Table 2.[26]

Acknowledgments

Financial support of this work by the Deutsche Forschungsgemeinschaft and the Fonds der Chemischen Industrie is gratefully acknowledged.

[1] B. K. Burgess, D. J. Lowe, *Chem. Rev.* **1996**, *96*, 2983–3011.
[2] J. B. Howard, D. C. Rees, *Chem . Rev.* **1996**, *96*, 2965–2982.
[3] R. R. Eady, *Chem. Rev.* **1996**, *96*, 3013–3030.
[4] [4a] D. Sellmann, J. Utz, N. Blum, F. W. Heinemann, *Coord. Chem. Rev.* **1999**, *190–192*, 607–627. – [4b] R. N. F. Thorneley, D. J. Lowe, J. Biolog. *Inorg. Chem.* **1996**, *1*, 576–580. – [4c] I. Dance, *J. Biolog. Inorg. Chem.* **1996**, *1*, 581–586. – [4d] D. Sellmann, J. Sutter, *J. Biolog. Inorg. Chem.* **1996**, *1*, 587–593. – [4e] D. Coucouvanis, *J. Biolog. Inorg. Chem.* **1996**, *1*, 594–600. – [4f] C. J. Rickett, *J. Biolog. Inorg. Chem.* **1996**, *1*, 601–606. – [4g] G. J. Leigh, *Eur. J. Biochem.* **1995**, *229*, 14–20.
[5] D. Sellmann, T. Gottschalk-Gaudig, F. W. Heinemann, *Inorg. Chem.* **1998**, *37*, 3982–3988 and literature cited therein.
[6] D. Sellmann, I. Barth, F. Knoch, M. Moll, *Inorg. Chem.* **1990**, *29*, 1822–1826.
[7] D. Sellmann, K. Engl, T. Gottschalk-Gaudig, F. W. Heinemann, *Eur. J. Inorg Chem.* **1999**, 333–339.
[8] F. Bottomley, in *A Treatise on Dinitrogen Fixation* (Eds.: R. W. F. Hardy, F. Bottomley, R. C. Burns), Wiley, New York, **1979**, p. 109–167.
[9] J. Chatt, D. P. Meloille, R. L. Richards, *J. Chem. Soc.* **1969**, 2841–2844.
[10] D. Sellmann, H. Kunstmann, F. Knoch, M. Moll, *Inorg. Chim. Acta* **1988**, *154*, 157–167.
[11] D. Sellmann, A. Hennige, *Angew. Chem.* **1997**, *108*, 270–271; *Angew. Chem. Int. Ed. Engl.* **1997**, *36*, 276–278.
[12] [12a] D. Sellmann, E. Böhlen, M. Waeber, G. Huttner, L. Zsolnai, *Angew. Chem.* **1985**, *97*, 984–985; *Angew. Chem. Int. Ed. Engl.* **1985**, *24*, 981–982. – [12b] D. Sellmann, J. Käppler, F. Knoch, M. Moll, *Inorg. Chem.* **1993**, *32*, 960–964.
[13] [13a] D. Sellmann, J. Sutter, *Acc. Chem. Res.* **1997**, *30*, 460–469. – [13b] D. Sellmann, J. Sutter, in "Transition Metal Sulfur Chemistry: Biological and Industrial Significance" (Eds.: E. I. Stiefel, K. Matsumoto), *ACS Symp. Ser.* **1996**, *653*, 101–116. – [13c] D. Sellmann, T. Becker, F. Knoch, *Chem. Eur. J.* **1996**, *2*, 1092–1098.
[14] T. Gottschalk-Gaudig, Dissertation, University Erlangen-Nürnberg, **1997**, p. 94–96.
[15] D. Sellmann, T. Gottschalk-Gaudig, F. W. Heinemann, *Inorg. Chim. Acta* **1998**, *269*, 63–72.
[16] N. N. Greenwood, A. Earnshaw, *Chemie der Elemente*, VCH Weinheim, **1988**, p. 546.
[17] M. Koepp, H. Wendt, H. Strehlow, *Z. Elektrochem.* **1960**, *64*, 483–491.
[18] M. Regitz, *Chem. Ber.* **1966**, *99*, 3128–3147.
[19] J. Thiele, *Justus Liebigs Ann. Chem.* **1892**, *271*, 127.
[20] I. P. Evans, A. Spencer, G. Wilkinson, *J. Chem. Soc., Dalton Trans.* **1973**, 204–209.
[21] H. Schmidbaur, G. Blaschke, *Z. Naturforsch.* **1980**, *35b*, 584–587.
[22] D. Sellmann, W. Weber, *J. Organomet. Chem.* **1986**, *304*, 195–205.
[23] H. Hope, in *Experimental Organometallic Chemistry* (Eds.: Al L. Wayda, M. Y. Darensbourg), *ACS Symp. Ser.* **1987**, *357*, 257–262.
[24] R. H. Blessing, *Acta Crystallogr.* **1995**, *A51*, 33–37.
[25] *SHELXTL 5.03 for Siemens Crystallographic Research Systems*, Siemens Analytical X-ray Instruments Inc., Madison, WI, USA, **1995**.
[26] Crystallographic data (excluding structure factors) for the structures reported in this paper have been deposited with the Cambridge Crystallographic Data Centre as CCDC-133763 (**7**), -133764 (**13**·CH_2Cl_2), -133765 (**16**·CH_2Cl_2), -133766 (**18**·4THF), -133767 (**19**·4CH_2Cl_2). Copies of the data can be obtained free of charge on application to The Director, CCDC, 12 Union Road, Cambridge CB2 1EZ, UK [Fax: (internat.) + 44-1223/336-033, E-mail: deposit@ccdc.cam.ac.uk].

Received November 9, 1999
[I99400]